

Drug response prediction by ensemble learning and drug-induced gene expression signatures*

Mehmet Tan ^{†1}, Ozan Fırat Özgül¹, Batuhan Bardak¹, Işıksu Eksioğlu¹, and Suna Sabuncuoğlu²

¹Department of Computer Engineering, TOBB University of Economics and Technology, Ankara, Turkey

²Toxicology Department, Faculty of Pharmacy, Hacettepe University, Ankara, Turkey

Abstract

Chemotherapeutic response of cancer cells to a given compound is one of the most fundamental information one requires to design anti-cancer drugs. Recent advances in producing large drug screens against cancer cell lines provided an opportunity to apply machine learning methods for this purpose. In addition to cytotoxicity databases, considerable amount of drug-induced gene expression data has also become publicly available. Following this, several methods that exploit omics data were proposed to predict drug activity on cancer cells. However, due to the complexity of cancer drug mechanisms, none of the existing methods are perfect. One possible direction, therefore, is to combine the strengths of both the methods and the databases for improved performance. We demonstrate that integrating a large number of predictions by the proposed method improves the performance for this task. The predictors in the ensemble differ in several aspects such as the method itself, the number of tasks method considers (multi-task vs. single-task) and the subset of data considered (sub-sampling). We show that all these different aspects contribute to the success of the final ensemble. In addition, we attempt to use the drug screen data together with two novel signatures produced from the drug-induced gene expression profiles of cancer cell lines. Finally, we evaluate the method predictions by *in vitro* experiments in addition to the tests on data sets. The predictions of the methods, the signatures and the software are available from <http://mtan.etu.edu.tr/drug-response-prediction/>.

Keywords: drug signatures, cell line signatures, drug response prediction, ensemble learning

1 Introduction

The highly variable nature of treatment responses among cancer patients necessitate tailor-made therapies. Forecasting the most feasible drug therapy for an individual patient, being the vital part of such personalized therapies, is a gruelling task since it requires the application of several candidate drugs on cancer on an individual basis. Determining chemotherapeutic response of malign cells *in silico* is an important problem whose solution can greatly contribute to both drug discovery and to such personalized treatment design. Several recently introduced large scale drug screen databases provided a significant opportunity to train machine learning models that predict drug activity (Garnett et al., 2012; Barretina et al., 2012). These databases provide data based on a large number of cytotoxicity experiments treating cancer cell lines with chemicals. Accurate

*This research was supported by The Scientific and Technological Research Council of Turkey (Grant no:115E274)

[†]Corresponding author:mtan@etu.edu.tr

machine learning models exploiting these databases have the potential to replace some of the wet-lab experiments performed for these different procedures.

There are several recent studies on drug sensitivity and anti-cancer drug response prediction. In (Wan and Pal, 2014), random forest regression model was used for obtaining a single drug or a group of drugs for a certain cancer. (Zhang et al., 2015) proposes an approach with cell line similarity network (CSN) and drug similarity network (DSN) data to predict anti-cancer drug responses of a given cell line by using dual-layer integrated cell line-drug network. To predict drug activity, (Turki and Wei, 2017) proposes a novel approach that uses link prediction algorithms and compare their results with existing drug sensitivity prediction models. Based on their experimental results, link prediction algorithms perform better than the methods used in comparison. Multi-task learning schemes have come into prominence as a consequence of their capability of exploiting inter-drug relationships during training. While multi-task learning for the drug activity prediction was largely limited to regularized linear models before, recently more sophisticated approaches have emerged. An approach called Kernelized Bayesian Multi-task Learning (KBMTL) (Gonen and Margolin, 2014) relying on kernel-based dimension reduction and multi-task learning demonstrated notable performance for drug response prediction. The study by Tan (Tan, 2016) has shown that the trace-norm regularized multi-task learning followed by a kernel transform of the input gene expression data is superior to several other methods proposed for this task. A similar work by Yuan et al (Yuan et al., 2016), also demonstrates the improved predictive power of multi-task learning with trace-norm regularization. In another study (Wang et al., 2017), the authors premeditates that the similar drugs should possess similar responses and define drug-similarity by Pearson correlation of drug responses. This is followed by application of a novel method called similarity-regularized matrix factorization (SRMF) which maps drugs and cell lines to a lower dimensional space and reconstruct the drug response matrix in this latent space. The usage of ensemble methods were also found promising in drug response prediction task, as in many other problems. These low-variance models surpassed all other schemes in a recent DREAM challenge on predicting human responses to toxic compounds (Eduati et al., 2015). Winners of both sub-tasks utilized ensemble of random forest models where each forest was devoted to a single cluster of cell lines. In addition to ensemble learning, biologically-plausible preprocessing techniques such as filtrating irrelevant genetic features, clustering cell lines and chemical using external datasets were found to be efficient strategies. None of these methods consider to use both multi-task and single-task methods together in an ensemble model. Also none considered to integrate the LINCS database to the transcriptional profiles for this task.

Our contributions in this paper can be summarized as follows. First, we propose to use an ensemble model to predict cytotoxicity of anti-cancer drugs by using four different prediction methods. Three of these methods have been recently proposed for this task, and the last one is a multi-task neural network. For each of these, similar cell lines and drugs are grouped and a large number of models are trained on these subsets of data as in the winning strategy for DREAM challenge (Eduati et al., 2015). We, then, combine the predictions from these models into a single prediction by stacked generalization. Second, we propose cell line sensitivity and drug activity signatures by integrating multiple databases and study the effect of these to the response prediction performance. Finally, we validate the predictions *in vitro* by treating one cell line with five selected compounds. The results are promising; both the ensemble model and signatures improve the prediction performance compared to the baseline methods.

In the following sections, we first describe the data sets that we use. Then, Section 3 discusses the drug activity and cell line sensitivity signatures and Section 4 provides the details on the proposed ensemble method. Finally, we report the experimental results in Section 5 and conclude in Section 6.

2 Datasets

The first database that we use is the Genomics of Drug Sensitivity in Cancer (GDSC) database (Iorio et al., 2016). More than a thousand cancer cell lines were screened against a large number of anti-cancer therapeutics. The main aim of the source is to identify biomarkers that lead to drug sensitivity or resistance. The cell lines are characterized in multiple omics features such as the gene expression, copy number variation and coding variants. We utilize the gene expression data as there is a wide consensus that this is the most informative data type for drug response prediction (Costello et al., 2014). Gene expression data is produced by Affymetrix Human Genome U219 Array and normalized by robust multiarray averaging (RMA). Second database that we utilize is the Cancer Cell Line Encyclopedia (CCLE) (Barretina et al., 2012). This is a similar screen to GDSC where the mRNA expression data is produced by using AffyMetrix U133+2 arrays. Provided data is the perturbational profile of 504 cancer cell lines treated with 24 anti-cancer drugs. Gene expression profiles provided by GDSC and CCLE is high-dimensional; the number of genes is around 17000. To reduce dimension, we applied the gene selection procedure we previously proposed in (Tan, 2016), where the number of genes selected is 1274 and 1239 for CCLE and GDSC respectively. The last database we use, Library of Integrated Network-based Cellular Signatures (LINCS), is composed of drug-induced gene expression profiles of the cancer cell lines (Subramanian et al., 2017). The database has recently been enlarged and moved to a new home called the CMAP L1000 database¹. The database currently holds perturbational profiles of tens of cell lines treated with tens of thousands of perturbagens most of which are small molecules. The profiles are given in terms of 978 landmark genes that can explain most of the variance in the gene expression profile of a cell line. In this paper we used the LINCS Phase II version by using the provided API.

3 Signatures

This section describes the proposed signatures to represent the activity and sensitivity of the drugs and cell lines, respectively.

3.1 Drug activity signatures

Lincscld API provides access to the experimental results in Library of Integrated Network-based Cellular Signatures (LINCS)² Program database. This database exhibits the effect of a drug on numerous cell lines by means of up or down regulations of landmark genes chosen by the database curators. We use these experimental results with the aim of generating drug activity signatures which represents each drug by its induced gene expression changes.

The first step of drug activity signature generation is the formation of experimental signatures, $ExpSig(dr, CL)$, that represents the gene-specific changes on a cell line CL upon application of drug dr in vector form:

$$ExpSig(dr, CL) = \langle gene_1 \uparrow, gene_2 \downarrow, gene_3 \downarrow, \dots, gene_K \uparrow \rangle \quad (1)$$

where the arrows represent the up and down regulations for the genes.

For a given drug dr and cell line CL , $ExpSig(dr, CL)$ can be constructed by a single LINCS access, where the database API provides the most regulated 50 genes.

¹<http://clue.io>

²<http://www.lincsproject.org/>

Experimental signatures are generated for all cell line-drug pairs in our dataset. In the LINCS database, multiple experiments can exist for a given cell line-drug pair with different experimental parameters such as dose and duration. For instance, there are 188 different experiments for cell line MCF7 treated with Vorinostat, where we considered these as distinct experiments.

Based on the experiment signatures ($ExpSig$), drug activity signature ($ActSig$) that represents the cumulative gene expression changes induced by a drug dr is defined as follows:

$$ActSig(dr) = \bigcup_{CL} ExpSig(dr, CL) \quad (2)$$

where, \bigcup_{CL} represents the combination of the experiment signatures for dr over all experiments involving dr in LINCS. Here, combination can be performed in several different ways. We define combination as the number of experiments for which the genes are up and down regulated. Therefore,

$$ActSig(dr) = \langle g_1(\uparrow n_1^u, \downarrow n_1^d), \dots, g_K(\uparrow n_K^u, \downarrow n_K^d) \rangle \quad (3)$$

The notation $g_1(\uparrow n_1^u, \downarrow n_1^d)$, states that dr is observed to up-regulate gene g_1 in n_1^u experiments and it down-regulates g_1 in n_1^d experiments.

$ActSig$ defined here, therefore, represents how a drug effects the cell lines, where this can be considered as an expression of mode of action (MOA) for a drug, in terms of gene regulations. $ActSig$ also has the property of decreasing the effect of experimental errors by averaging over several experiments.

3.2 Cell line sensitivity signatures

While GDSC and CCLE databases include the cytotoxicity measurements of compounds on particular cell lines, LINCS database exhibits differential gene expression profiles of cell lines upon treatment with a large number of compounds. By a cell line sensitivity signature (CLSS) we aim to gather the gene expression changes in a cell line CL , induced by different compounds. However, we restrict these compounds to be the ones that are found to be active against CL , where the activity information is extracted from other pharmacological screening studies such as GDSC. By this restriction, our purpose is to build a signature that describes drug-induced differential gene expression in the cell lines which are sensitive to those drugs (hence the name 'sensitivity signature').

Building the CLSS for a cell line is initiated by selecting an activity threshold, T , for the considered activity measure (IC_{50} in our case). Then, for all the (dr, CL) pairs with IC_{50} below T , we query the LINCS database to retrieve the up or down regulated landmark genes. Querying LINCS for (dr, CL) pair leads to three different possible scenarios: (i) LINCS might include (dr, CL) experiment and experimental results can be directly used, (ii) (dr, CL) experiment might not have been performed in LINCS, despite the existence of dr and/or CL . In this case, the experimental results of dr applied on cell lines similar to CL can be used, (iii) dr may not be available in LINCS. In this last case, if the (known) target proteins of dr have been used in gene knock-out experiments in LINCS, their results on cell lines similar to CL can be used to approximate the drug effect. Formally, the result of this procedure that we call the sensitivity signature (SensSig) can be defined as follows.

$$SensSig(dr, CL) = \begin{cases} ExpSig(dr, CL) & (dr, CL) \in \text{LINCS} \\ ActSig(dr) & dr \in \text{LINCS and } (dr, CL) \notin \text{LINCS} \\ & \text{(on similar cell lines to } CL) \\ TargetSig(Targets_{dr}) & dr \notin \text{LINCS (on similar cell lines to } CL) \end{cases} \quad (4)$$

where we used \in to denote inclusion in database for ease of notation and $TargetSig(Targets_{dr})$ corresponds to case (iii) above, differential gene expression profile for the gene knock-out experiments for the targets of dr , $Targets_{dr}$.

As mentioned above, CLSS aims to cover the differential gene expression profile leading to cell death in tumour cells. $SensSig(dr, CL)$ describes the profile in response to dr only. As there can be a large number of experiments on CL in LINCS, combination of $SensSig(dr, CL)$ over all drugs applied on CL can describe the cumulative gene expression changes that are critical for CL . Based on this, we define CLSS as follows,

$$CLSS(CL) = \bigcup_{dr} SensSig(dr, CL) \quad (5)$$

The combination \bigcup_{dr} in the above equation can be defined in a number of different ways. This can simply be a set union. However, the one which we think can better represent the cumulative sensitivity, is to construct CLSS as a set of vectors, where each vector corresponds to the union of signatures over drugs targeting the same pathway. The target pathway information for each compound is obtained from GDSC. This way we will have a number of signatures for each cell line corresponding to the target pathways of the drugs in Equation 5.

3.3 Signature similarities

As mentioned above, the two signatures defined above characterize the cell lines and drugs in terms of sensitivity and activity respectively. The sensitivity signature is a representation of the gene expression changes that lead to cell death in a certain cell line. Similarly, drug activity signature is a representation of the "mode of action" for a drug, summarizing the cumulative differential gene expression upon treatment on cell lines. Therefore, a natural next step is to compare these signatures to predict whether a given drug is active on a given cell line.

This approach is similar to the connectivity score of the Connectivity Map (CMAP) (Lamb et al., 2006) (the previous version of LINCS) for drug repositioning. The connectivity score defined in CMAP also compares two differential gene expression signatures to find a drug that has the effect of reverting the expression profile back to normal. CMAP finds and outputs the drugs whose effect is the opposite of a given differential gene expression profile for a certain condition (a disease for example). Our ultimate goal here, on the other hand, is to directly predict the drug activity. To this aim, we propose to use the similarity between the proposed drug and cell line signatures to be able to "help" some other methods to better predict drug response. In other words, we are looking for the drugs that will kill most of the malignant cells in a certain tumor.

To sum up, we hypothesize that the matching between $CLSS(CL)$ and $ActSig(dr)$ should give us a clue on the activity of the drug dr on the cell line CL . For this, we used cosine similarity between the signatures, where, among other choices, we observed that it performed better. As each $CLSS$ is a list of vectors (corresponding to different pathways), we computed the similarity of each vector in $CLSS(CL)$ with $ActSig(dr)$ and used the maximum of these as the similarity between the sensitivity of CL and the activity of dr . So from here on, we will refer this maximum value when we use the term "signature similarity".

4 Ensemble model for drug activity prediction

There can be multiple motivations to build ensembles as listed in (Dietterich, 2000); statistical, representational and computational. All these different aspects more or less contribute to the motivation of the work in this paper. Despite recent improvements in availability of drug response data, amount of data can still cause multiple different hypotheses to perform reasonably well, and combining them can improve the performance. Also, we do not yet know the best representation for drug response models which can differ for each individual drug, therefore an ensemble with different representation assumptions, again, might help. Computational aspect seems to contribute less than the formers to the motivation, however as the available data increase, we think it can become equally important as well.

Cancer types may substantially differ in aspects such as development, behavior and response to treatment. In order to handle this in the method, we also exploit some form of subsampling by clustering the cell line samples. One possible effect of this operation is to reduce the variance error. The other is to model the more closely related cancer types together, which can make the predictive models more stable and focused to certain types of cancer. In addition, to combine the outputs of multiple models, stacking technique with different meta-learners is used. Following subsections detail the proposed ensemble method. The whole method that we call Ensemble Learning for Drug Activity Prediction (ELDAP) is summarized in Figure 1. We will refer the ELDAP method that does not exploit the signatures in stacking as ELDAP\S.

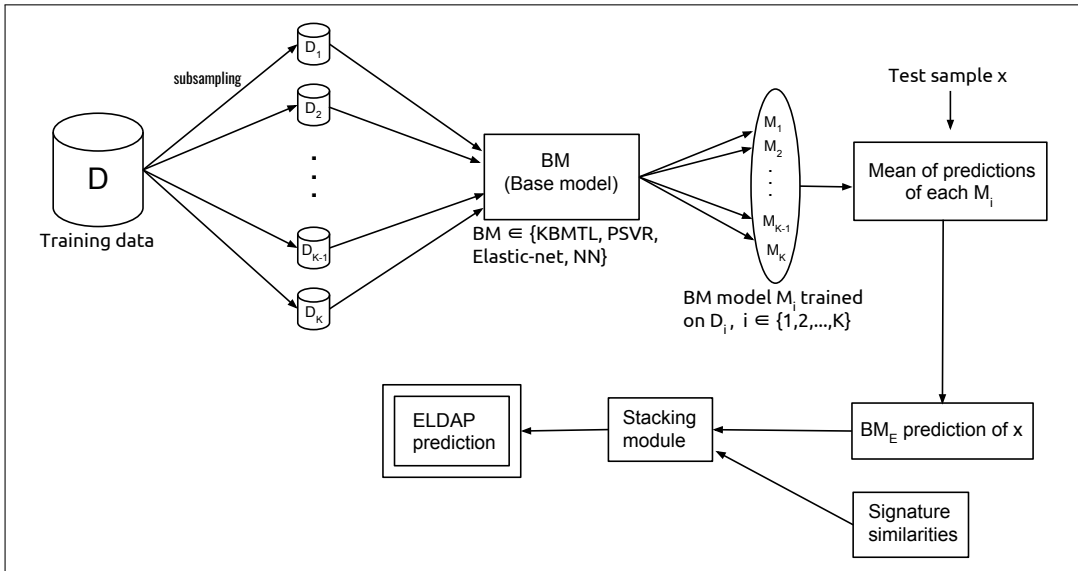


Figure 1: Block diagram for the ELDAP method. The prediction of ELDAP is the output of a stacking module, where the input to the stacking module is the output of base model ensembles. Some details are omitted in this figure, further details are given in the text.

4.1 Base regressors

This section defines the base models that we use as the learning methods in ensemble learning. These four are selected based on their previous use or their potential to be successful for this problem.

Elastic Net: Elastic Net Regression which combines ridge and Lasso regression is a popular sparse regularized learning method. In genomics datasets, where number of features are typically larger

than the number of samples, sparsity is a desired property. Elastic Net outputs a matrix W that minimizes the following error function:

$$\frac{1}{2n} \|Y - XW\|_2^2 + \alpha(\rho \|W\|_1 + (1 - \rho) \|W\|_2^2) \quad (6)$$

The α parameter sets the weight for the regularization. ρ balances the lasso and ridge penalty and n is the number of samples. These parameters were chosen as the ones minimizing the cross-validation error on a separate grid search. We used Elastic-net as a single task method where it is the form that was previously applied on GDSC for biomarker detection successfully (Garnett et al., 2012).

Kernelized Bayesian Multitask Learning: Kernelized Bayesian Multitask Learning (KBMTL) (Gonen and Margolin, 2014) aims at solving related tasks jointly through a multitask regression scheme followed by a kernelized non-linear dimensionality reduction stage. The multitask algorithm reveals the shared information between distinct tasks in the kernel space and generates joint models. Such a procedure is capable of eliminating drug-specific noise as well as off-target effects. Moreover, joint modeling enables to utilize missing data since the regression is performed over a large set of data rather than individual data points. This property makes KBMTL a useful tool for genomics data where scarcity is a serious issue. KBMTL optimization procedure includes determining the hidden representations of data points in the kernel subspace and projection matrices.

Pairwise support vector regression: We call a support vector machine (SVM) a pairwise support vector regressor (PSVR) when the input data are composed of objects including two (possibly different) elements and the target is continuous. Depending on the task, a sample, therefore, usually represents an interaction or relationship between the elements. In our case, each sample is a drug-cell line pair and the target is the IC_{50} value. This has been applied to a similar classification task before (Tan, 2014). We follow here a similar procedure with the difference that our task here is a regression task. A similar approach was carried out also in protein-ligand interaction prediction (Jacob and Vert, 2008) and in compound toxicity prediction (Bernard et al., 2017).

We define a pairwise kernel K_p as the product of the drug kernel K_d and the cell line kernel K_c .

$$K_p((dr_j, CL_i), (dr_l, CL_k)) = K_d(dr_j, dr_l) * K_c(CL_i, CL_k) \quad (7)$$

where both K_d and K_c are defined as the radial basis function (RBF) kernel between the drug and cell line descriptors, respectively. The descriptors that we use for drugs are the PaDEL descriptors (Yap, 2011), and the gene expression profile of the selected subset of genes for the cell lines.

Neural networks: Artificial Neural Networks are one of the most widely used models in machine learning. With recent advancements in graphics processing units and training methods remarkable achievements have been witnessed in speech recognition, image understanding and machine translation. For an introduction and recent developments, see (Goodfellow et al., 2016). In this paper, we used a multi-layer feed forward neural network with a multi-task output layer. The architectural details for the network that we use is given in Section 5.

4.2 Learning Strategy for base models

We have followed a novel learning strategy with the intent of exploiting sample similarities. Instead of training a model or an ensemble of models trained on the whole training set, we

generated several smaller training subsets corresponding to the neighborhood of a certain training sample.

This training process can be summarized as follows: A single training sample is chosen and together with its 300 closest neighbours in the training set, we form a subset. 300 is chosen as the best performing value out of a set of neighborhood values. The distance metric defining the neighborhood of a sample is the Pearson correlation of the gene expression data. Due to the relatively small number of samples, with the target values this constitutes a highly underdetermined system. To resolve this problem, we computed the Radial Basis Function (RBF) kernel gram matrix for all the methods except the PSVR. In this way, submatrix becomes a symmetrical square matrix where each index reflects the RBF similarity between two samples. This not only performs a non-linear transformation, but also reduces the dimension. The models are trained on this newly formed gram matrix. We construct submatrices this way from the training set which, after training, results in a model corresponding to each sample. The testing of new samples is straightforward. When a test sample, which is a gene expression profile characterizing a cell line, arrives, the most similar 300 training cell lines and associated models are identified. The mean value of the predictions of this collection of models is returned as the overall predicted IC_{50} value.

4.3 Stacked generalization

Stacked generalization (or stacking) method where individual predictions of a collection of models are introduced as inputs to a second-level learning algorithm is an extensively used technique for boosting prediction accuracy (Wolpert, 1992). In our work, we blended Elastic Net, KBMTL, Neural Networks and PSVR through a stacking module. Although, stacking only aims at blending previously made predictions, addition of newer features to the process is also possible. As previously stated, we hypothesize that employing cell-line/drug signatures at the second level can augment the accuracy. For this purpose, we generated a new feature called signature similarity which is defined by the cosine similarity between drug and cell-line signatures. This feature is computed for all cell-line and drug pairs for which the signatures could be computed.

The main challenge of designing a second-level learner for blending was the missing values. Due to the amount of intersection between databases, we could acquire signature similarity metrics only for 133 drugs and 45 cell lines which approximately corresponds to 2.5 % of the original dataset. Therefore, we attempted to implement stacking schemes where signature similarity values contribute to the results only when they are available. This was a challenging task where the proposed models were supposed to be robust to changing input characteristics, e.g. missing/present signature similarity values. We propose three strategies, each satisfying these conditions. These can be splitted into three categories:

(i) *Simple model averaging*: Here, the predictions of the individual models were averaged with and without weighting. When used, the weights were chosen as being inversely proportional to individual models' MSEs on the data. In other words, a model making better predictions alone had more contribution in the average, as well. It is noteworthy that the signature similarities could not be directly included in the averaging since they did not represent IC_{50} values but similarities. Therefore, prior to averaging, we utilized a pre-learner responsible for mapping signature similarities to IC_{50} values. This pre-learner was chosen among a set of models including linear regression, support vector regression and regression tree. The choice and the tuning of this model were based on cross-validation.

(ii) *Conventional machine learning models*: Though variable input characteristics hampered the usage of classical machine learning models in a straight-forward way, it was still possible to train a different model for each input setting. For instance, one could train a regression tree model for observations with all possible features such as individual predictions and signature similarities,

while turning to a new regression tree model for the samples lacking any of these features. For this class, we included models such as support vector machines, regression trees and shallow neural networks.

(iii) *Modified distance-based models*: The last category of methods were the adaptive models which could dynamically adapt themselves to the changing input environments. In this class, we only included distance-based models since average inter-sample distances could be computed even in the absence of specific features. For this purpose, we designed a modified KNN regressor measuring the distances only based on the available features.

For both data sets, we aimed to obtain the lowest MSE by varying these stacking strategies. It should be noted that, this process was fully automated, a meta-learner or combination of multiple meta-learners minimizing the cross-validation error was chosen from the bag of candidate models. Same models were tested with and without signature similarity values so as to confirm the effect of similarities during prediction. For GDSC dataset, the lowest MSE values were achieved as the average of two stacking modules; a modified KNN (iii) and model averaging (i). It should be noted that the signature similarities were transformed into IC₅₀ values by a linear model. In CCLE dataset, an averaging module with a regression tree pre-learner was the most successful. No further averaging was found to be efficient. The effect of signature similarities was evaluated by comparing the MSE of indices, e.g. cell line-drug pairs, with available signature similarity values. We iterated the prediction process with and without signature similarities on these indices and observed the improvement when similarities were utilized.

5 Experimental Results

In this section we report the experimental results corresponding to two different evaluations. In the first part, we report the results of the cross validation (CV) experiments that we name as *in silico* experiments. The second part gives the results of *in vitro* experiments of the selected cell line and drugs.

5.1 *In silico* evaluation

For the *in silico* evaluation, all the reported results are the average mean squared errors of a 3-fold CV. The experiments were performed on a computer with 3.2GHz CPU and 16GB of RAM running Linux. Here, for each compound, there is a vector of cytotoxicity values corresponding to the target vector of a learning problem. We refer to the drug activity prediction problem composed of a set of samples and one of these target vectors, as a task here. The performance of a task is measured in terms of the task specific mean squared error (TMSE);

$$TMSE(t) = \frac{1}{n} \sum_{i=1}^n (\hat{y}_i^t - y_i^t)^2 \quad (8)$$

for a given task t , where n is the number of samples and \hat{y}_i^t and y_i^t are the predicted and correct cytotoxicity values for task t and sample i , respectively. The overall performance is reported as the mean TMSE (MSE):

$$MSE = \frac{1}{T} \sum_{t=1}^T TMSE(t) \quad (9)$$

where T is the number of tasks.

For each of the methods, we optimized the method parameters with a separate grid search. As a result of that, the parameters that we use are as follows. For Elastic-net, we used $\alpha = 0.01$ and $\rho = 1$ (which means that the method actually performs a Lasso regression). We used the scikit-learn (Pedregosa et al., 2012) library for the implementation of Elastic-net. For KBMTL, we set $\{\alpha_\lambda, \beta_\lambda, \alpha_\epsilon, \beta_\epsilon, R, \sigma_h, \sigma_w\} = \{1, 1, 1, 1, 20, 0.1, 1\}$. We executed KBMTL for 200 iterations. The author provided implementation was used for KBMTL. For neural network, we used two hidden layers with Rectified Linear Unit activations. For each hidden layer we used a dropout rate of 0.5. The size of the two hidden layers are 270 and 200 respectively. We used the stochastic gradient descent optimizer with a learning rate of 0.01 and applied a batch size of 100. We used Keras library (Chollet, 2015) for the implementation.

We report the results in five steps. In the first part, the performances of the single methods are given in Table 1a. These results are reported as the baseline results for comparison. Due to the scalability issues of SVMs, the results for PSVR could not be reported for GDSC, as the run lasted for more than two weeks. For CCLE, as the data set is smaller, the performance of PSVR is also reported and it seems to be the best among others. However, one also should note that PSVR uses the extra information of compound structures. Also, as mentioned before, the number of compounds with available structure data is 21 and 224 for CCLE and GDSC, respectively. One should take this into account for performance comparison. Among single methods, KBMTL significantly outperforms other methods for GDSC.

In the second step of the results we report in Table 1b, the performances of the single method ensembles (see Section 4.2) are given. We mark these methods with a subscript E for readability as in Figure 1. Except PSVR, for each method, we observe a performance improvement compared to Table 1a. Also note that, the improvement for Elastic-net is the largest. The performance difference is significant for Elastic-net and NN for GDSC. However it is not possible to confirm statistically that the improvements are significant for CCLE.

The third part of the results report the overall performance of ELDAP and ELDAP\S in Table 2a. We can not see a performance improvement here, as the ratio of cell lines and drugs that have the signatures available is low. To demonstrate the effect of signatures, therefore, we report the results for the ones with signatures only. In this case, a small improvement can be observed (see Table 2b). We also provide some literature based evidence for some pairs with highly similar signatures in last part of this section. The fourth part of the results correspond to the drug specific errors. For each drug, we show the errors in Figure 2 and 3 for GDSC and CCLE respectively. As it is seen in figures, the performance of ELDAP is superior in almost all drugs, especially for GDSC. Note that Figures 2 and 3 compare the single method performances (Table 1a) with ELDAP (Table 1b).

So far, we presented the efficiency and reliability of generated signature similarity metrics by only inferring the augmented prediction accuracy when they are included in the stacking stage. However, pharmacological inferences are also possible. In this section, we attempt to relate our results with the literature on specific drug activities. For this purpose, we randomly select few cell line-drug pairs among the ones with very high/low signature similarity scores, e.g. the best and the worst 5. Among this short list, the most enhanced pattern is domination of few specific drugs on several cell lines. In other words, the independent from the cell lines they are applied to, some drugs achieved the highest signature similarity scores. Majority of these successful drugs were observed to target major pathways enhancing cancer cell proliferation such as ERK/MAPK signaling and PI3K/MTOR signaling. Apart from these, drugs regulating cell cycles and apoptosis through cyclin depending kinases (CDK2, CDK7, CDK9) and caspase activators (Procaspase-3, Procaspase-7), respectively, were also present among the most successful drugs. The last set of drugs found among the top-tier drugs were growth factor receptor inhibitors obstructing IGF1R signalling (IGF1R, IR) and thus cancer cell proliferation. Obtaining high signature similarity results on these targeted drugs acting on the most important pathways linked

	GDSC	CCLE
KBMTL	2.030±0.150	4.496±1.125
PSVR	-	3.768±0.587
Elastic-net	2.571±0.150	5.694±0.924
NN	2.464±0.271	4.408±0.726

(a) Single methods

	GDSC	CCLE
KBMTL _E	2.064±0.150	4.073±0.522
PSVR _E	2.518±0.205	4.806±1.040
Elastic-net _E	2.015±0.171	4.233±0.736
NN _E	2.040±0.156	4.087±0.695

(b) Single method ensembles

Table 1: Performance of the single methods and single method ensembles

	GDSC	CCLE
ELDAP\S	1.808±0.142	3.928±0.606
ELDAP	1.808±0.142	3.928±0.606

(a) Overall performance

	GDSC(Sig)	CCLE(Sig)
ELDAP\S	1.880±0.553	1.840±0.544
ELDAP	1.971±0.773	1.816±0.687

(b) Performance on signature sub-matrix

Table 2: Performance of ELDAP

to cancer cell survival is biologically sensible and an indicator of reasonability of our signature-based approach.

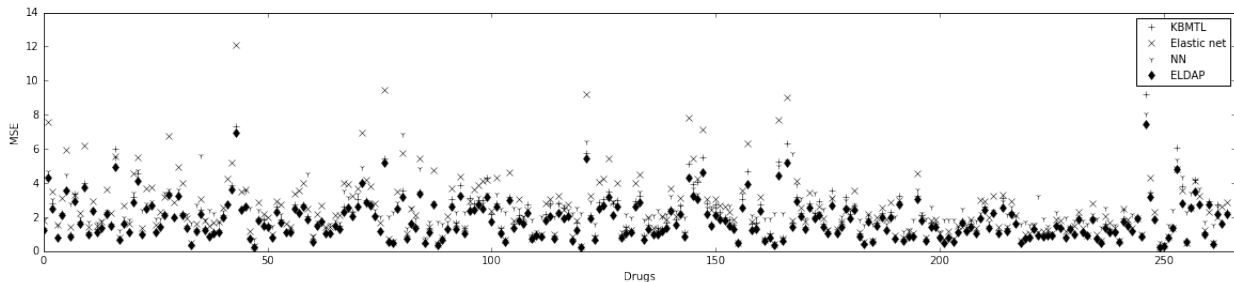


Figure 2: Drug specific errors for the GDSC data set.

5.2 *In vitro* evaluation

In addition to the *in silico* evaluation, we performed *in vitro* evaluation on a cancer cell line. We selected A549, human epithelial lung carcinoma cell line, as our *in vitro* test bed. Other than the availability of the cell line, this choice is arbitrary. Five different compounds were selected that were not applied on A549 in the GDSC dataset. The selection was done by checking the error rates in the *in silico* evaluation of the compounds and cytotoxicity variance of the drugs. The compounds are the ones that have the smallest error rates and largest variances (as variance can be considered an indicator of selectivity) among the commercially available chemicals. A549 was treated with these five different compounds and the resulting cytotoxicity values were compared to the predictions by the proposed method. Following subsections give the results and further details of these wet-lab experiments.

5.2.1 Chemicals

The chemicals and reagents used in the experiments were purchased from the following suppliers: Fetal calf serum (FCS), trypsin-EDTA, Dulbecco’s modified Eagle’s medium (DMEM), penicillin-streptomycin, L-glutamine from Biological Industries (Kibbutz Beit-Haemek, Israel);

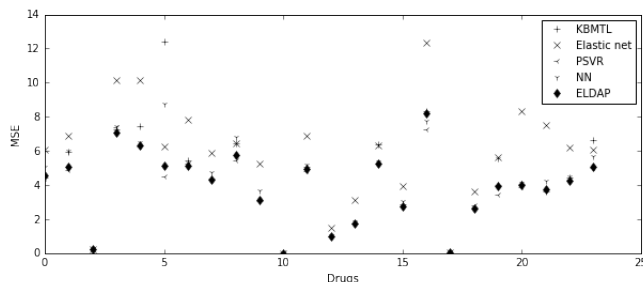


Figure 3: Drug specific errors for the CCLE data set.

3-(4,5-dimethylthiazol-2-yl)-2,5-diphenyltetrazolium bromide (MTT) dye, methylene blue dye, methanol (MEOH), from Merck Chemicals (Darmstadt, Germany); dimethyl sulfoxide (DMSO), ethanol, from ICN Biomedicals Inc. (Aurora, Ohio, USA).

5.2.2 Cell culture

A549 cells, human epithelial lung carcinoma cell line, were purchased from American Type Culture Collection (Manassas, VA, USA). The cells were maintained in DMEM containing 10% fetal calf serum and 0,5% penicillin-streptomycin. The cells were kept in a incubator (Thermo Scientific Heraeus, Germany) at $37 \pm 1^\circ\text{C}$ with a humidified atmosphere of 95% air and 5% CO_2 . The culture medium was changed two times in one week. A549 cells used in all experiments were between the 2nd and 3rd culture passage after thawing.

5.2.3 Determination of cytotoxicity by MTT assay

The effects of the compounds, TAK-715, GSK2126458, Ispinesib mesylate, KIN001-102 and OSI-930 on cell viability were determined by MTT assay with slight changes described by (Ohguro et al., 1999). A549 cell line is highly sensitive and has good characteristics in colony formation. Therefore these adherent cells are very convenient for MTT assay. Before starting experiments, the cells have been grown for 2 weeks. Afterwards A549 cells were seeded at density of 5000 and 10000 cells/well in 96-well plates and allowed to grow for 24 h before treatment. The cells were treated with each compounds at different concentrations (0.0064, 0.032, 0.16, 0.8, 4, 20, 100, 500 μM for TAK-715, KIN001-102, OSI-930 and 0.00128, 0.0064, 0.032, 0.16, 0.8, 4, 20, 100 μM for GSK2126458, Ispinesib mesylate) in the culture medium for 48 h and 72 h. The compounds were dissolved in DMSO and added to the medium to yield a final DMSO concentration of 1% (v/v). Control group cells were treated with the culture medium containing 1% of DMSO without compounds. Following the incubation period, the medium was removed and 1 mg/mL MTT solution in 100 μL of the culture medium was added to each well and further incubated at 37°C for 3 h. After the MTT application, the medium was discarded, and 100 μL of PBS was added to wash the cells. 100 μL of DMSO was added onto the cells in order to dissolve the formazan crystals. Absorbance of each sample was measured at 570 nm using the microplate reader (SpectraMax M2, Molecular Devices Limited, Berkshire, UK). Cytotoxic potential of the compounds were determined by calculating the percentage of cell viability ratio between treated and untreated (control) cells (% cell viability) IC_{50} values of the drugs was calculated by using the dose-response curves. Each experiment was performed in triplicate.

5.2.4 Evaluation of cytotoxic effects of the compounds on A549 cell line

The cytotoxic effects of the compounds at different concentrations on A549 cell line are shown in Figure 4 and 5. According to the results, the compounds showed significant cytotoxicity on A549 cell line. The concentration-dependent cytotoxicity was observed for A549 cells after both 48 h and 72 h exposure to the compounds.

The IC_{50} values of cytotoxic drugs were calculated as explained in Section 5.2.3 and shown in Table 3 and 4. The *in vitro* results were compared to the predictions of ELDAP for all compounds. The predictions of ELDAP for these drugs are shown in Table 5. As it is shown in Table 3 and 4 the IC_{50} values of the compounds are inline with IC_{50} predictions in Table 5. Note that one should not expect an exact match with the predictions here as there are significant differences in experimental conditions though we did our best to build a similar wet-lab environment that the GDSC data set is produced.

Drug	IC_{50} (48 h)	IC_{50} (72 h)
TAK 715	40.53	3.32
GSK 2126458	17.74	0.10
Ispinesib Meylate	3.63	1.63
KIN001-102	13.26	5.01
OSI-930	370.31	65.34

Table 3: The IC_{50} (μ M) values of the compounds for A549 cells with 5000 cell/well at 48h and 72 h

Drug	IC_{50} (48 h)	IC_{50} (72 h)
TAK 715	32.39	18.40
GSK 2126458	3.22	0.03
Ispinesib Meylate	3.63	3.77
KIN001-102	19.02	17.05
OSI-930	368.56	403.67

Table 4: The IC_{50} (μ M) values of the compounds for A549 cells with 10000 cell/well at 48h and 72 h

Drug	Predicted cytotoxicity
TAK 715	106.738
GSK 2126458	0.071
Ispinesib Meylate	0.285
KIN001-102	21.716
OSI-930	69.036

Table 5: Predicted cytotoxicity values by ELDAP

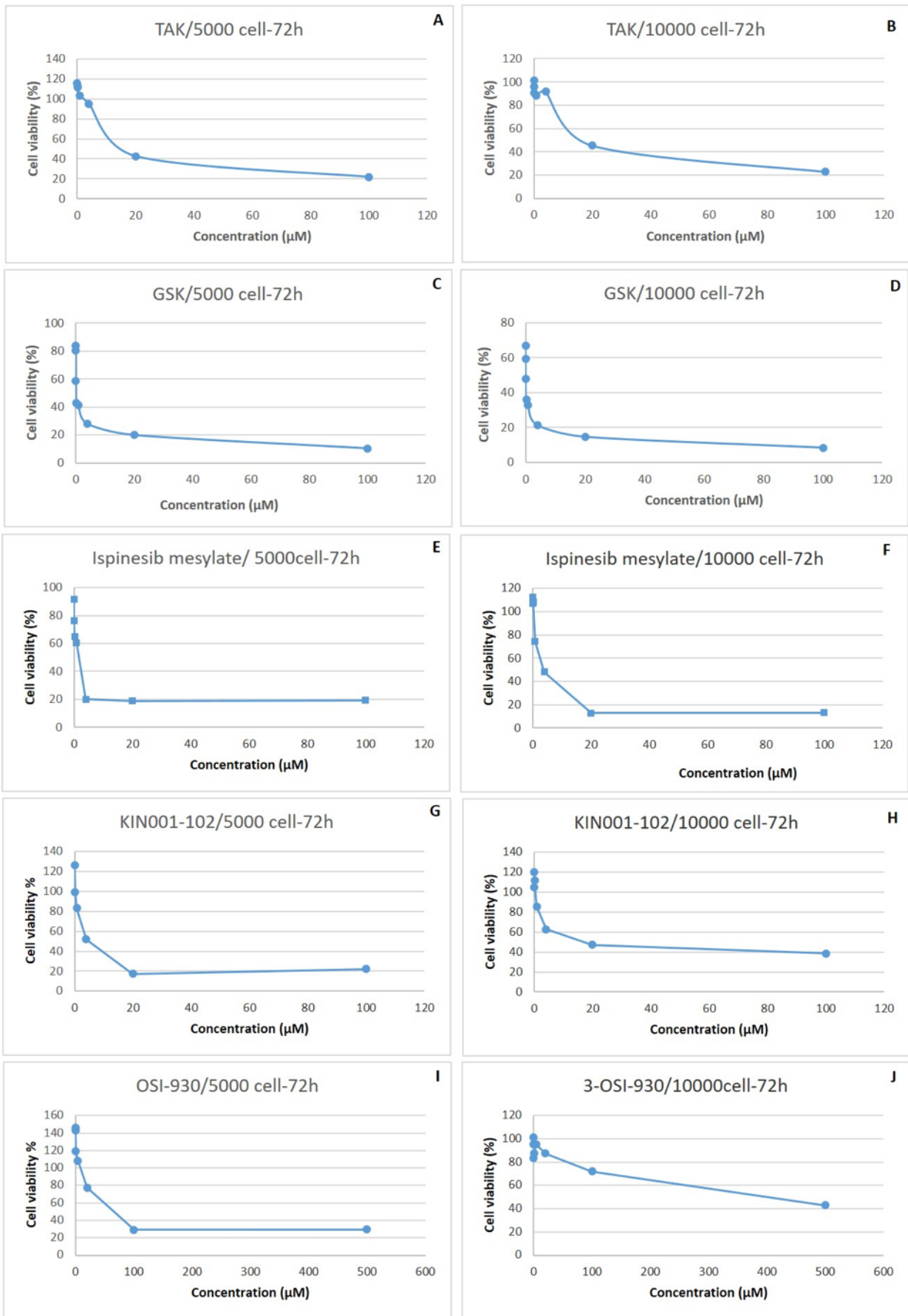


Figure 4: Effects of the compounds on cell viability of A549 cells with 5000 cell/well (A, C, E, G, I) or 10000 cell/well (B, D, F, H, J) for 48 h exposure.

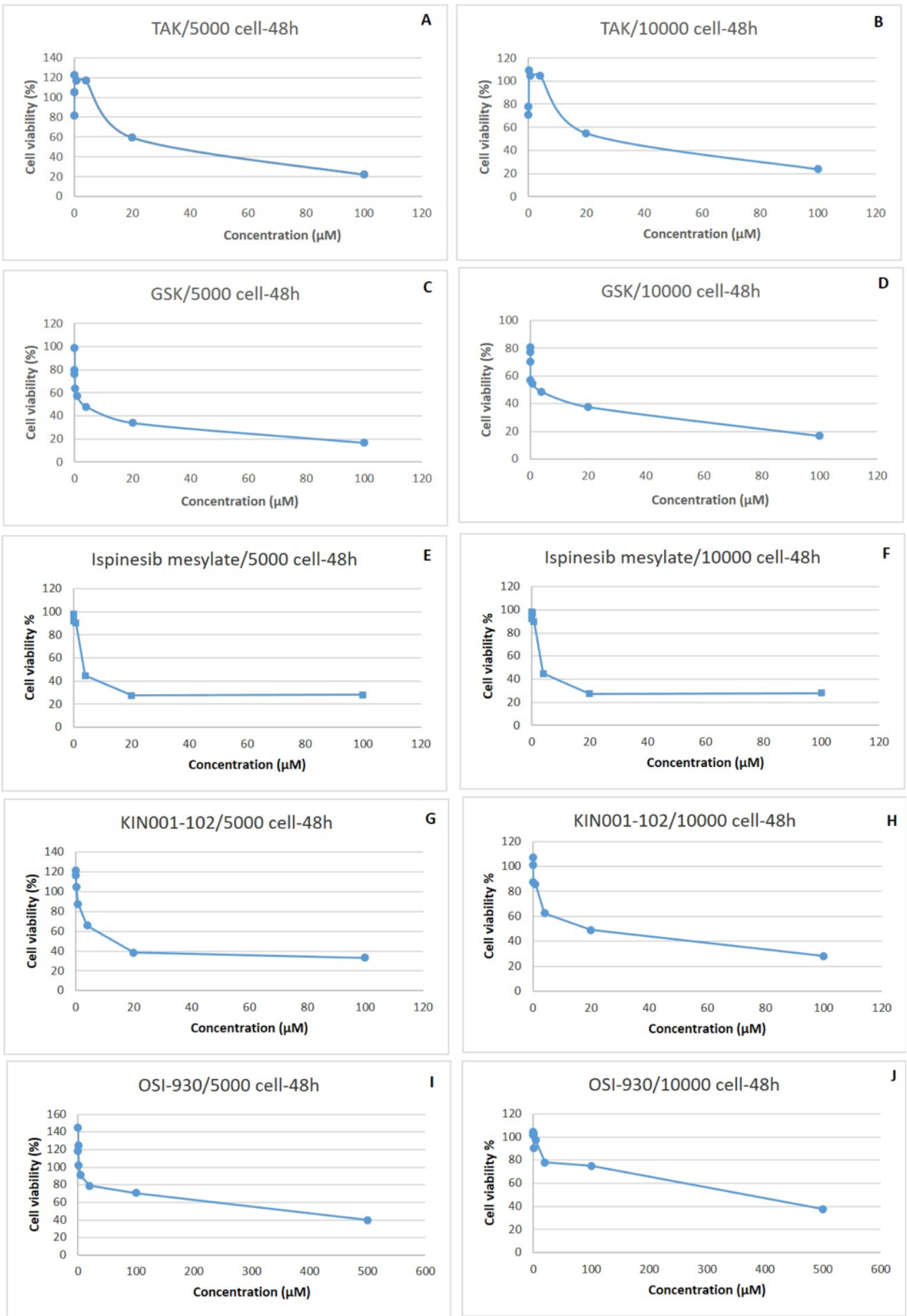


Figure 5: Effects of the compounds on cell viability of A549 cells with 5000 cell/well (A, C, E, G, I) or 10000 cell/well (B, D, F, H, J) for 72 h exposure.

6 Conclusion

Prediction of chemotherapeutic response of malign cells is an essential part of designing personalized drugs. Recent efforts of producing large scale data sets provides the opportunity to apply machine learning models to this problem.

In this paper we proposed an ensemble learning method which combines both multi-task and single task learners through a stacking module. We demonstrated the usage of novel signatures that represent the activity and sensitivity of drugs and cell lines, respectively. These signatures are defined in a way that the similarity between them can be used as an indicator of drug activity for the corresponding cell line. In addition to the computer based evaluation, *in vitro* experiments performed on cell line A549 for 5 drugs depicted that the method can produce reliable predictions. The small number of drugs in the intersection of LINCS and the other databases, GDSC and CCLE, limited the efficacy of the signature similarities. In case of the data availability, the significance of the effect can be more clearly demonstrated.

Several directions can be followed to extend this work. One is to incorporate new data types that can effect the results, such as the pathway data sets. The pathway information can help in selecting the genes in the same pathway for modeling. Another usage can be to exploit the pathway cancer relationship in the sense that only related genes can be used in the sub-models. This can be further extended in case the cell lines are grouped by their tissue or cancer type. Another possible extension is to apply active learning techniques to this problem, where the next wet-lab experiment to perform can be selected in such a way that the new cytotoxicity value is maximally effective on improving the prediction performance. We believe that this kind of a cycle can greatly decrease the error rates.

References

- Jordi Barretina, Giordano Caponigro, Nicolas Stransky, Kavitha Venkatesan, Adam A. Margolin, Sungjoon Kim, Christopher J. Wilson, Joseph Lehár, Gregory V. Kryukov, Dmitriy Sonkin, Anupama Reddy, Manway Liu, Lauren Murray, Michael F. Berger, John E. Monahan, Paula Morais, Jodi Meltzer, Adam Korejwa, Judit Jané-Valbuena, Felipa A. Mapa, Joseph Thibault, Eva Bric-Furlong, Pichai Raman, Aaron Shipway, Ingo H. Engels, Jill Cheng, Guoying K. Yu, Jianjun Yu, Peter Aspesi, Melanie De Silva, Kalpana Jagtap, Michael D. Jones, Li Wang, Charles Hatton, Emanuele Palesscandolo, Supriya Gupta, Scott Mahan, Carrie Sougnez, Robert C. Onofrio, Ted Liefeld, Laura MacConaill, Wendy Winckler, Michael Reich, Nanxin Li, Jill P. Mesirov, Stacey B. Gabriel, Gad Getz, Kristin Ardlie, Vivien Chan, Vic E. Myer, Barbara L. Weber, Jeff Porter, Markus Warmuth, Peter Finan, Jennifer L. Harris, Matthew Meyerson, Todd R. Golub, Michael P. Morrissey, William R. Sellers, Robert Schlegel, and Levi A. Garraway. The Cancer Cell Line Encyclopedia enables predictive modelling of anticancer drug sensitivity. *Nature*, 483(7391):603–607, 2012. ISSN 00280836. doi: 10.1038/nature11003. URL <http://dx.doi.org/10.1038/nature11003>.
- Elsa Bernard, Yunlong Jiao, Erwan Scornet, Veronique Stoven, Thomas Walter, and Jean Philippe Vert. Kernel Multitask Regression for Toxicogenetics. *Molecular Informatics*, 2017. ISSN 18681751. doi: 10.1002/minf.201700053.
- François Chollet. Keras, 2015. URL <https://github.com/fchollet/keras>.
- James C Costello, Laura M Heiser, Elisabeth Georgii, Mehmet Gönen, Michael P Menden, Nicholas J Wang, and et al. A community effort to assess and improve drug sensitivity prediction algorithms. *Nature biotechnology*, 32(12):1–103, 2014. doi: 10.1038/nbt.2877. URL <http://www.ncbi.nlm.nih.gov/pubmed/24880487>.

- T G Dietterich. Ensemble methods in machine learning. In *Multiple Classifier Systems. First International Workshop, MCS 2000. Proceedings (Lecture Notes in Computer Science Vol.1857)*, 2000.
- Federica Eduati, Lara M. Mangravite, Tao Wang, Hao Tang, J. Christopher Bare, Ruili Huang, Thea Norman, Mike Kellen, Michael P. Menden, Jichen Yang, Xiaowei Zhan, Rui Zhong, Guanghua Xiao, Menghang Xia, Nour Abdo, Oksana Kosyk, Stephen Friend, Allen Dearry, Anton Simeonov, Raymond R. Tice, Ivan Rusyn, Fred A. Wright, Gustavo Stolovitzky, Yang Xie, Julio Saez-Rodriguez, Tero Aittokallio, Salvatore Alaimo, Alicia Amadoz, Muhammad Ammad-ud din, Chloé Agathe Azencott, Jaume Bacardit, Pelham Barron, Elsa Bernard, Andreas Beyer, Shao Bin, Alena van Bömmel, Karsten Borgwardt, April M. Brys, Brian Caffrey, Jeffrey Chang, Jungsoo Chang, Himanshu Chheda, Eleni G. Christodoulou, Mathieu Clément-Ziza, Trevor Cohen, Marianne Cowherd, Sofie Demeyer, Joaquin Dopazo, Joel D. Elhard, Andre O. Falcao, Alfredo Ferro, David A. Friedenberg, Rosalba Giugno, Yunguo Gong, Jenni W. Gorospe, Courtney A. Granville, Dominik Grimm, Matthias Heinig, Rosa D. Hernansaiz, Petheri Hintsanen, Sepp Hochreiter, Liang Chin Huang, Matthew Huska, Alok Jaiswal, Yunlong Jiao, Samuel Kaski, Ismeet Kaur, Suleiman Ali Khan, Günter Klambauer, Natalio Krasnogor, Michael Kuhn, Miron Bartosz Kurska, Rintu Kutum, Nicola Lazzarini, Inhan Lee, Michael K.K. Leung, Weng Khong Lim, Charlie Liu, Felipe Llinares López, Alessandro Mammanna, Andreas Mayr, Tom Michoel, Misael Mongiovì, Jonathan D. Moore, John Patrick Mpindi, Ravi Narasimhan, Stephen O. Opiyo, Gaurav Pandey, Andrea L. Peabody, Juliane Perner, Antti Poso, Alfredo Pulvirenti, Konrad Rawlik, Susanne Reinhardt, Carol G. Riffle, Douglas Ruderfer, Aaron J. Sander, Richard S. Savage, Erwan Scornet, Patricia Sebastian-Leon, Roded Sharan, Carl Johann Simon-Gabriel, Veronique Stoven, Jingchun Sun, Jing Tang, Ana L. Teixeira, Albert Tenesa, Jean Philippe Vert, Martin Vingron, Thomas Walter, Krister Wennerberg, Sean Whalen, Zofia Wisniewska, Yonghui Wu, Hua Xu, Shihua Zhang, Junfei Zhao, W. Jim Zheng, and Dai Ziwei. Prediction of human population responses to toxic compounds by a collaborative competition. *Nature Biotechnology*, 33(9):933–940, 2015. ISSN 15461696. doi: 10.1038/nbt.3299.
- Mathew J Garnett, Elena J Edelman, Sonja J Heidorn, Chris D Greenman, Anahita Dastur, King Wai Lau, and et al. Systematic identification of genomic markers of drug sensitivity in cancer cells. *Nature*, 483:570–575, 2012.
- M. Gonen and A. A. Margolin. Drug susceptibility prediction against a panel of drugs using kernelized Bayesian multitask learning. *Bioinformatics*, 30(17):i556–i563, 8 2014. ISSN 1367-4803. doi: 10.1093/bioinformatics/btu464. URL <http://bioinformatics.oxfordjournals.org/content/30/17/i556.short>.
- Ian Goodfellow, Yoshua Bengio, and Aaron Courville. Deep Learning–book. *MIT Press*, 521 (7553):800, 2016. ISSN 0028-0836. doi: 10.1038/nmeth.3707. URL <http://goodfeli.github.io/dlbook/><http://dx.doi.org/10.1038/nature14539>.
- Francesco Iorio, Theo A. Knijnenburg, Daniel J. Vis, Graham R. Bignell, Michael P. Menden, Michael Schubert, Nanne Aben, Emanuel Gonçalves, Syd Barthorpe, Howard Lightfoot, Thomas Cokelaer, Patricia Greninger, Ewald van Dyk, Han Chang, Heshani de Silva, Holger Heyn, Xianming Deng, Regina K. Egan, Qingsong Liu, Tatiana Mironenko, Xeni Mitropoulos, Laura Richardson, Jinhua Wang, Tinghu Zhang, Sebastian Moran, Sergi Sayols, Maryam Soleimani, David Tamborero, Nuria Lopez-Bigas, Petra Ross-Macdonald, Manel Esteller, Nathanael S. Gray, Daniel A. Haber, Michael R. Stratton, Cyril H. Benes, Lodewyk F.A. Wessels, Julio Saez-Rodriguez, Ultan McDermott, and Mathew J. Garnett. A Landscape of Pharmacogenomic Interactions in Cancer. *Cell*, 2016. ISSN 10974172. doi: 10.1016/j.cell.2016.06.017.

- Laurent Jacob and Jean-philippe Vert. Protein – ligand interaction prediction : an improved chemogenomics approach. *Bioinformatics*, 24(19):2149–2156, 2008. doi: 10.1093/bioinformatics/btn409.
- Justin Lamb, Emily D Crawford, David Peck, Joshua W Modell, Irene C Blat, Matthew J Wrobel, Jim Lerner, Jean-philippe Brunet, Aravind Subramanian, Kenneth N Ross, Michael Reich, Haley Hieronymus, Guo Wei, Scott a Armstrong, Stephen J Haggarty, Paul a Clemons, Ru Wei, and Steven a Carr. The Connectivity Map : Using. *Science*, 2006. ISSN 1095-9203. doi: 10.1126/science.1132939.
- N Ohguro, M Fukuda, T Sasabe, and Y Tano. Concentration dependent effects of hydrogen peroxide on lens epithelial cells. *British Journal of Ophthalmology*, 1999.
- Fabian Pedregosa, Gaël Varoquaux, Alexandre Gramfort, Vincent Michel, Bertrand Thirion, Olivier Grisel, Mathieu Blondel, Peter Prettenhofer, Ron Weiss, Vincent Dubourg, Jake Vanderplas, Alexandre Passos, David Cournapeau, Matthieu Brucher, Matthieu Perrot, and Édouard Duchesnay. Scikit-learn: Machine Learning in Python. *Journal of Machine Learning Research*, 12:2825–2830, 2012. ISSN 15324435. doi: 10.1007/s13398-014-0173-7.2. URL <http://dl.acm.org/citation.cfm?id=2078195%5Cnhttp://arxiv.org/abs/1201.0490>.
- Aravind Subramanian, Rajiv Narayan, Steven M. Corsello, David D. Peck, Ted E. Natoli, Xiaodong Lu, Joshua Gould, John F. Davis, Andrew A. Tubelli, Jacob K. Asiedu, David L. Lahr, Jodi E. Hirschman, Zihan Liu, Melanie Donahue, Bina Julian, Mariya Khan, David Wadden, Ian C. Smith, Daniel Lam, Arthur Liberzon, Courtney Toder, Mukta Bagul, Marek Orzechowski, Oana M. Enache, Federica Piccioni, Sarah A. Johnson, Nicholas J. Lyons, Alice H. Berger, Alykhan F. Shamji, Angela N. Brooks, Anita Vrcic, Corey Flynn, Jacqueline Rosains, David Y. Takeda, Roger Hu, Desiree Davison, Justin Lamb, Kristin Ardlie, Larson Hogstrom, Peyton Greenside, Nathanael S. Gray, Paul A. Clemons, Serena Silver, Xiaoyun Wu, Wen Ning Zhao, Willis Read-Button, Xiaohua Wu, Stephen J. Haggarty, Lucienne V. Ronco, Jesse S. Boehm, Stuart L. Schreiber, John G. Doench, Joshua A. Bittker, David E. Root, Bang Wong, and Todd R. Golub. A Next Generation Connectivity Map: L1000 Platform and the First 1,000,000 Profiles. *Cell*, 2017. ISSN 10974172. doi: 10.1016/j.cell.2017.10.049.
- Mehmet Tan. Drug sensitivity prediction for cancer cell lines based on pairwise kernels and miRNA profiles. In *Proceedings - 2014 IEEE International Conference on Bioinformatics and Biomedicine, IEEE BIBM 2014*, 2014. ISBN 9781479956692. doi: 10.1109/BIBM.2014.6999145.
- Mehmet Tan. Prediction of anti-cancer drug response by kernelized multi-task learning. *Artificial Intelligence in Medicine*, 73:70–77, 2016. doi: 10.1016/j.artmed.2016.09.004.
- Turki Turki and Zhi Wei. A link prediction approach to cancer drug sensitivity prediction. *BMC Systems Biology*, 11(Suppl 5):94, 10 2017. ISSN 1752-0509. doi: 10.1186/s12918-017-0463-8. URL <http://www.ncbi.nlm.nih.gov/pmc/articles/PMC5629619/>.
- Qian Wan and Ranadip Pal. An Ensemble Based Top Performing Approach for NCI-DREAM Drug Sensitivity Prediction Challenge. *PLoS ONE*, 9(6), 2014. ISSN 19326203. doi: 10.1371/journal.pone.0101183.
- Lin Wang, Xiaozhong Li, Louxin Zhang, and Qiang Gao. Improved anticancer drug response prediction in cell lines using matrix factorization with similarity regularization. *BMC Cancer*, 17(1):513, 2017. ISSN 1471-2407. doi: 10.1186/s12885-017-3500-5. URL <http://bmccancer.biomedcentral.com/articles/10.1186/s12885-017-3500-5>.

- David H. Wolpert. Stacked generalization. *Neural Networks*, 1992. ISSN 08936080. doi: 10.1016/S0893-6080(05)80023-1.
- Chun Wei Yap. PaDEL-descriptor: An open source software to calculate molecular descriptors and fingerprints. *Journal of Computational Chemistry*, 32(7):1466–1474, 2011.
- Han Yuan, Ivan Paskov, Hristo Paskov, Alvaro J. González, and Christina S. Leslie. Multi-task learning improves prediction of cancer drug sensitivity. *Scientific Reports*, 6(1):31619, 2016. ISSN 2045-2322. doi: 10.1038/srep31619. URL <http://www.nature.com/articles/srep31619>.
- Naiqian Zhang, Haiyun Wang, Yun Fang, Jun Wang, Xiaoqi Zheng, and X. Shirley Liu. Predicting Anticancer Drug Responses Using a Dual-Layer Integrated Cell Line-Drug Network Model. *PLoS Computational Biology*, 11(9), 2015. ISSN 15537358. doi: 10.1371/journal.pcbi.1004498.